IC/88/223

INTERNATIONAL CENTRE FOR THEORETICAL PHYSICS

A PHENOMENOLOGICAL AND APPROXIMATELY FLAVOUR INDEPENDENT POTENTIAL FOR QUARK-ANITQUARK SYSTEM

Xiaotong Song

INTERNATIONAL ATOMIC ENERGY AGENCY

UNITED NATIONS EDUCATIONAL, SCIENTIFIC AND CULTURAL ORGANIZATION

International Atomic Energy Agency
and
United Nations Educational Scientific and Cultural Organization

INTERNATIONAL CENTRE FOR THEORETICAL PHYSICS

A PHENOMENOLOGICAL AND APPROXIMATELY FLAVOUR INDEPENDENT POTENTIAL FOR QUARK-ANTIQUARK SYSTEM *

Xiaotong Song **
International Centre for Theoretical Physics, Trieste, Italy.

ABSTRACT

We proposed a phenomenological and flavour independent potential for quark-antiquark systems with equal or unequal masses. The potential has a Lorentz vector term motivated by empirical formula of leptonic width of vector meson at short distances and a Lorentz scalar part inspired by the result from lattice QCD responsible for quark confinement at large distances. Using this potential we calculated the energy levels, leptonic widths, radiative transition rates and hadronic decay rates of the $(u\bar{u})$, $(d\bar{d})$, $(s\bar{s})$, $(c\bar{c})$, $(b\bar{b})$ and $(t\bar{t})$ systems. The fine and hyperfine splittings of light and heavy quark-antiquark systems are also calculated. Most results agree fairly well with the experiment.

MIRAMARE - TRIESTE
August 1988

* To be submitted for publication.
This paper is a contribution to the XXIV International Conference on High Energy Physics, Munich, 4-10 August, 1988.

** Permanent address: Hangzhou University, Hangzhou, People's Republic of China.

1. INTRODUCTION

Since the discovery of the charmonium system, the non-relativistic potential model has been successfully used to describe the heavy quarkonium spectroscopy and decay. By using various theoretical effective potentials many detailed studies have been made [1 - 15]. These investigations have provided lots of important information about the dynamical nature of quark interactions expected from quantum chromodynamics [25 -28].

Recently, we suggested a phenomenological potential for heavy quarkonium [16]

$$U(r) = -br^{-1/2} + ar^{1/2} \tag{1}$$

which consists of a Lorentz vector part $V(r) = -br^{-1/2}$ motivated by the experimental leptonic widths of vector mesons

$$\Gamma(V \to e^+e^-)/e_Q^2 \simeq 12 \text{ Kev} \tag{2}$$

and a Lorentz scalar part $S(r) = ar^{1/2}$ responsible for quark confinement. Most results are thus improved.

However, there still remain many problems, some of which we will study in this paper. 1) When we used $ar^{1/2}$ to reflect the average effects of the many channel coupling, the choice of power 1/2 was a bit arbitrariness, and the potential $r^{1/2}$ seems increasing not fast enough with r to reproduce the level spacing for the higher excited states of the charmonium. 2) Although potential (1) has been rather successful for the heavy mesons $(c\bar{c})$, $(b\bar{b})$ and presumably $(t\bar{t})$, we do not know whether they can also give a good description of light mesons. Since Martin [17], Richard [18] and other authors [19 - 21] have been able to obtain

good results for states involving the s-quark, it is natural to consider the extension of our phenomenological potential to light mesons consisting of the s-, d- and u-quarks. In other words, we hope to know whether we can obtain a unified treatment of light and heavy mesons within the framework of phenomenological potential model. In fact, a lot of investigations on this subject have been made by many authors [15, 22-24].

In this paper, we suggest an improved square root potential and present the results of a study of light and heavy mesons in which the quark and antiquark masses may or may not be equal. Our result shows that all mesons can be fairly well described by nonrelativistic model with a phenomenological and approximately flavor-independent potential. Section 2 describes our improved potential. In section 3, and section 4, we calculate the spectroscopy and various decay rates. Discussion and comments of our results and particularly for hyperfine splitting of mesons are given in section 5.

2. AN IMPROVED SQUARE ROOT POTENTIAL

If we believe that the quark potential model is a reasonable model for low energy hadron phenomenology and adopt the view of effective potential we can use nonrelativistic quantum mechanics to study the energy levels and decay rates of hadrons. Although quantum chromodynamics is widely believed to be the correct theory of the quark interactions, we have not yet obtained a basic understanding of quark confinement. We thus have to rely on potential model and often use the ideas from QCD to motivate the asymptotic behavior of the potential in two limits: $r \to 0$ and $r \to \infty$.

At short distances one loop QCD calculation leads to a softened Coulomb-like potential [7] $U(r) \xrightarrow[r \to 0]{} 1/r\ln r$. The two-loop QCD calculation shows that the singularity of the potential at r=0 will be softened further [10]. An interesting question is whether the calculation including corrections to all orders in QCD can lead to a more strongly softened potential and what is the form of this potential if which does exist. As we discussed in our previous paper [16], from the empirical relation (2) and Van Royen and Weisskopf formula for leptonic width of vector meson, an inverse square root potential $V(r) = -r^{-1/2}$ has been suggested. In this paper we are not going to change this behavior of potential at short distances.

Concerning the form of the potential at larger distances the situation is even much more complicated. Qualitatively, the potential would be strongly weakened by the screening effects due to the quark pair creation above threshold. In fact, the increasing of linear potential, $S(r) \sim r$, with r seems too fast so that the calculated leptonic widths of higher $c\bar{c}$ and $b\bar{b}$ excited states exceed the experimental data. Olsson and Suchyta III [30] discussed the spin-orbit contribution of the confining interaction and found that the confining potential must fall below linear potential. Most recently, the calculation of lattice QCD for baryon spectrum leads to an effective quark potential $V(r) = A\, r^{\epsilon}$ ($A = 0.508$, $\epsilon = 0.671$) [31], which also shows a potential weaker than linear which might be more suitable for describing effective quark interaction at large distance.

In this paper we will choose $r^{0.6}$ as our confinement potential.

Therefore we suggest an improved square root potential

$$U(r)= V(r) + S(r) = -br^{-0.5} + ar^{0.6} \tag{3}$$

and adjust two parameters a and b to reproduce the experimental levels of the n^3S_1 $c\bar{c}$ and $b\bar{b}$ states. We find

$$a = 1.0 \text{ GeV fm}^{-0.6}, \qquad b = 0.42 \text{ GeV fm}^{0.5} \tag{4}$$

and*

$$m_c= 1.7 \text{ GeV}/c^2, \qquad m_b= 5.2 \text{ GeV}/c^2 \tag{5}$$

A surprising thing is the phenomenological potential (3) which also gives a good description for light mesons provided taking a somewhat larger value of parameter b, and we find

$$a = 1.0 \text{ GeV fm}^{-0.6}, \qquad b' = 0.60 \text{ GeV fm}^{0.5} \tag{6}$$

and

$$m_u= m_d= 0.27 \text{ GeV}/c^2, \qquad m_s= 0.60 \text{ GeV}/c^2 \tag{7}$$

give fairly good fit to the spectroscopy of light mesons.

Since the role of the parameter b is, in some sense, similar to the QCD coupling constant α_s, $b' > b$ shows that the α_s for the light meson is larger than that for heavier one. This coincides with the asymptotic freedom of QCD.

3. ENERGY LEVELS, FINE AND HYPERFINE SPLITTINGS

The Hamiltonian of the quark-antiquark system is given by 3) 32)

$$H = H_o + H_I + m_1 + m_2 \tag{8}$$

* We can also take $m_c= 1.8 \text{ GeV}/c^2$ and $m_b= 5.0 \text{ GeV}/c^2$ as we did in 16), but the result shows that the calculated levels are not sensitive to the constituent masses.

where

$$H_o= p^2/2\mu + V(r) + S(r) \tag{9}$$

and

$$H_I= \frac{1}{2r}\left(\frac{\vec{L}\cdot\vec{s}_1}{m_1^2} + \frac{\vec{L}\cdot\vec{s}_2}{m_2^2}\right)\left(\frac{dV}{dr} - \frac{dS}{dr}\right)$$

$$+ \frac{\vec{L}\cdot\vec{S}}{m_1m_2r}\frac{dV}{dr} + \frac{S_{12}}{12m_1m_2}\left(\frac{1}{r}\frac{dV}{dr} - \frac{d^2V}{dr^2}\right)$$

$$+ \frac{1}{6m_1m_2}\left(\frac{d^2V}{dr^2} + \frac{2}{r}\frac{dV}{dr}\right)\vec{\sigma}_1\cdot\vec{\sigma}_2 \tag{10}$$

where m_1 and m_2 are quark and antiquark masses, μ is the reduced mass of the bound system. The tensor operator S_{12} is defined by

$$S_{12} = 3(\vec{\sigma}_1\cdot\hat{r})(\vec{\sigma}_2\cdot\hat{r}) - (\vec{\sigma}_1\cdot\vec{\sigma}_2) \tag{11}$$

and $\vec{\sigma}_i$ denotes the Pauli spin operators of i-th quark, $\vec{s}_i= \vec{\sigma}_i/2$. $\vec{L}$ is the relative angular momentum, $\vec{S}$ is the total spin operator. For equal masses, by perturbation we obtain

$$M(n^{2S+1}L_J) = 2m + E_{nL} + m_{LS}\langle\vec{L}\cdot\vec{S}\rangle + m_T\langle S_{12}\rangle + m_H\langle\vec{s}_1\cdot\vec{s}_2\rangle \tag{12}$$

where E_{nL} are the eigenvalues of zeroth order Schrödinger equation $H_o\,\psi_{nL} = E_{nL}\,\psi_{nL}$ and

$$m_{LS} = \frac{1}{2m^2}\left\langle\frac{1}{r}\left(\frac{dV}{dr} - \frac{dS}{dr}\right)\right\rangle = a_P \tag{13}$$

$$m_T = \frac{1}{12m^2}\left\langle\frac{1}{r}\frac{dV}{dr} - \frac{d^2V}{dr^2}\right\rangle = b_P \tag{14}$$

$$m_H = \frac{2}{3m^2}\left\langle\frac{d^2V}{dr^2} + \frac{2}{r}\frac{dV}{dr}\right\rangle \tag{15}$$

The calculated $c\bar{c}$ and $b\bar{b}$ energy levels are listed in Tables 1 and 2. One can see that the agreement with the data for higher excited states is indeed improved as compared with that from the original square root potential. The levels of $t\bar{t}$ for various top quark masses: m_t = 40, 45 and 50 GeV/c^2 are listed in Table 3.

For light mesons, using potential (3), with (6) and (7), the levels of $u\bar{u}$, $d\bar{d}$, $s\bar{s}$ and $u\bar{s}$, $d\bar{s}$ are also calculated and listed in Table 4. From the comparison of the theoretical values and the data we can see the agreement is fairly good.

For the mesons consisting of a heavy quark and a light antiquark, for instance $c\bar{u}$, $c\bar{d}$, $c\bar{s}$, $b\bar{u}$, $b\bar{d}$, $b\bar{s}$ and $b\bar{c}$ the lowest two levels for $^3S_1$ states are listed in Table 5. The parameter b are taken as follows

$$b' = 0.60 \text{ GeV fm}^{0.5} \quad \text{if } 2\mu < 1 \text{ GeV}/c^2 \quad (16)$$
(us, cu, cs, bu)

$$b = 0.42 \text{ GeV fm}^{0.5} \quad \text{if } 2\mu > 1 \text{ GeV}/c^2 \quad (17)$$
(bs, bc)

The comparison of the fine splitting of the ^3P_J states with experiment for $c\bar{c}$, $b\bar{b}$ and prediction for $t\bar{t}$ are listed in Table 6. The fine splitting coefficients a_P and b_P are listed in Table 7. We can see the agreement is good for $b\bar{b}$ but not for $c\bar{c}$.

Concerning the hyperfine splitting, it has been shown by some authors [33,34] that the difference between the mass squared of the vector meson and the mass squared of the corresponding pseudoscalar meson is approximately flavour-independent constant

$$\left[M_V(^3S_1)\right]^2 - \left[M_P(^1S_0)\right]^2 \simeq 0.56 \text{ GeV}^2 \quad (18)$$

But our result shows that $M_V^2 - M_P^2$ is a slowly-varying function of $\ln \mu_{ij}$ from $\rho\pi$ to D_s^*, D_s and increases very rapidly with $\ln \mu_{ij}$ for larger reduced masses as shown in Fig. 1. This result is similar to that of Igi and Ono [35].

The most interesting result is the dependence of hyperfine splitting $M_V - M_P$ on the variable $\ln(m_i+m_j)$. Fig. 2. shows that if we take $\ln(m_i+m_j)$ as a variable instead of $\ln \mu_{ij}$ data of $M_V - M_P$ presents a clear regularity [36]: hyperfine splitting decrease monotonically with increasing of $\ln(m_i+m_j)$.* It should be noted that if we take $\ln \mu_{ij}$ as a variable this regularity could not be seen (as shown in Fig. 3.). We will discuss this problem in section 5.

We also note that the hyperfine splitting is very sensitive to the short range part of the effective potential. For instance a change of b from 0.42 to 0.60 in V(r) leads to a change of $M_V - M_P$ for bs from 47.6MeV to 78 MeV. (see Table 8.)

* Except for $c\bar{c}$, in this case the predicted value is much less than the data. It might be due to neglecting the contribution of annihilation terms [38].

4. QUARKONIUM DECAY

A successful potential model for quarkonium should be able to describe not only the energy spectrum but also the decays via electroweak (photon, W- and Z^0-bosons) and strong (gluon) interactions.

1) Annihilation processes: which is sensitive to the $|\psi(0)|^2$ - the behavior of the wave function at small distances. These processes include leptonic decay, two-photon decay two-gluon annihilation (into hadrons) and three-photon decay and three-gluon annihilation.

a) Leptonic decay: The leptonic width for $^3S_1(Q\bar{Q}) \to \gamma^* \to e^+e^-$ including relativistic effects and two-loop QCD corrections is [37]

$$\Gamma(V\to e^+e^-) = \Gamma_{ee}^{(o)}(1-\beta^2/3)(1-16\alpha_s/3\pi + (24.26-0.11n_f)(\alpha_s/\pi)^2) \quad (19)$$

where [29]

$$\Gamma_{ee}^{(o)} = 16\pi\alpha^2 e_Q^2 \left|\psi_S(0)\right|^2/m_V^2 \quad (20)$$

Because there exists some ambiguities concerning relativistic and QCD corrections, we only discuss the ratios of the leptonic widths between n^3S_1 and 1^3S_1 states and assume these correction factors are roughly the same for different excited states in same family. The comparison of these ratios with the data and with other potential models for $c\bar{c}$ and $b\bar{b}$ are listed in table 1 and 2. The agreement for $b\bar{b}$ is good, but for $c\bar{c}$ the theoretical values are still higher than the data for the excited states higher than 2S.

b) The decay rates for two-photon and three-photon annihilation processes $(Q\bar{Q})\to 2\gamma$ and $(Q\bar{Q})\to 3\gamma$ are given by

$$\Gamma(n^1S_o \to 2\gamma) = 48\pi\alpha^2 e_Q^4 \left|\psi_{ns}(0)\right|^2/m_{ns}^2 \quad (21)$$

and

$$\Gamma(n^3S_1 \to 3\gamma) = (64/3)(\pi^2-9)\alpha^3 e_Q^6 \left|\psi_{ns}(0)\right|^2/m_{ns}^2 \quad (22)$$

c) The rates for two-gluon and three-gluon annihilation $(Q\bar{Q})\to 2g$ and $(Q\bar{Q})\to 3g$ are given by

$$\Gamma(n^1S_o \to 2g) = (32/3)\pi\alpha_s^2 \left|\psi_{ns}(0)\right|^2/m_{ns}^2 \quad (23)$$

and

$$\Gamma(n^3S_1 \to 3g) = (160/81)(\pi^2-9)\alpha_s^3 \left|\psi_{ns}(0)\right|^2/m_{ns}^2 \quad (24)$$

The rates for the process $(Q\bar{Q}) \to 2g$ (light hadron) $+\gamma$ are calculated from the following formula

$$\Gamma(n^3S_1 \to 2g+\gamma) = (128/9)(\pi^2-9)\alpha e_Q^2\alpha_s^2 \left|\psi_{ns}(0)\right|^2/m_{ns}^2 \quad (25)$$

where the QCD coupling constant α_s is calculated by using the two-loop expression [26]

$$\alpha_s(Q^2) = 4\pi\left[\beta_o \ln(Q^2/\Lambda^2) + (\beta_1/\beta_o)\ln(\ln(Q^2/\Lambda^2))\right]^{-1} \quad (26)$$

with

$$\beta_o = 11 - (3/2)n_f; \quad \beta_1 = 102 - (38/3)n_f$$
$$\Lambda = 100 \text{ MeV} \quad (27)$$

and $n_f = 3$ for $c\bar{c}$, $n_f = 4$ for $b\bar{b}$. We also assume that $Q^2 \simeq m_Q^2 \simeq m_{ns}^2/4$. The calculated results for all of these rates are listed in Table 9. The agreement between theoretical prediction and experiment is satisfactory.

d) Hadronic decay of ^3P_J states: The widths are given by [39]

$$\Gamma(^3P_0 \to 2g) = 384\pi\alpha_s^2 \left|\psi'_P(0)\right|^2 / m_0^4 \qquad (28)$$

$$\Gamma(^3P_2 \to 2g) = (4/15)\,\Gamma(^3P_0 \to 2g)\,(m_0/m_2)^4 \qquad (29)$$

and [40]

$$\Gamma(^3P_1 \to q\bar{q}g) = (512/3)\,\alpha_s^3 \left|\psi'_P(0)\right|^2 \ln(m/\Delta)/m_1^4 \qquad (30)$$

The comparison of theoretical widths with the data are listed in Table 10. The agreement for χ_b states is pretty good, but for χ_{2c} state the theoretical width is only 25% of the data.

2) Radiative transition: The electromagnetic process via one real photon emission, $(Q\bar{Q}) \to (Q\bar{Q})' + \gamma$, can be used to probe the behavior of the wave function at larger distances. The rates of electric dipole transition and magnetic dipole transitions of $(Q\bar{Q})$ states are given by

$$\Gamma(2^3S_1 \to 1^3P_J + \gamma) = (4/27)(2J+1)\alpha e_Q^2 k^3 \langle 1P|r|2S\rangle^2 \qquad (31)$$

$$\Gamma(1^3P_J \to 1^3S_1 + \gamma) = (4/9)\alpha e_Q^2 k^3 \langle 1S|r|1P\rangle^2 \qquad (32)$$

$$\Gamma(n^3S_1 \to n^1S_0 + \gamma) = (4/3)\alpha e_Q^2 k^3 \langle nS|j_0(kr)|nS\rangle^2/m_Q^2 \qquad (33)$$

where k is the momentum of the emitted photon and $k=(m_f^2-m_i^2)/2m_f$. The calculated widths for $c\bar{c}$ and $b\bar{b}$ are listed in Table 11. One can see the agreement of our results with the experiment is quite good. The prediction for $t\bar{t}$ is listed in Table 12.

5. SUMMARY AND DISCUSSION

1) We have suggested an improved square root potential(3) which has a short range behavior $r^{-0.5}$ motivated by experimental leptonic width of vector mesons and a confining part $r^{0.6}$ inspired by result from lattice QCD. Using the nonrelativistic wave equation and our potential with suitable parameters (4) - (7), we have calculated energy levels including fine and hyperfine splittings and various decay rates for $(u\bar{u})$, $(d\bar{d})$, $(s\bar{s})$, $(c\bar{c})$, $(b\bar{b})$ and $(t\bar{t})$ with equal masses, and for $(u\bar{d})$, $(u\bar{s})$, $(c\bar{u})$, $(c\bar{s})$, $(b\bar{u})$, $(b\bar{s})$ and $(b\bar{c})$ with unequal masses. Most results agree well with the experiment. It seems that we can, to some extent, obtain a unified treatment of light and heavy mesons within the framework of phenomenological potential model *.

2) We have computed $|\psi(0)|^2$ for various quarkonium states. the result shows (see Fig. 4)

$$|\psi(0)|^2 \sim \mu^{1.55 - 1.60} \qquad (34)$$

which agree well with the result given by some authors [42) 43)]. However, using (34) and formula (20) for leptonic width we can not get empirical relation (2). But recent data shows Γ_{ee}/e_Q^2 is not a flavor-independent constant (see Fig. 5). In fact, using (19) which includes relativistic and QCD radiative corrections we find that (34) gives a fairly good fit to the data from $\rho, \omega, \phi, J/\psi$ to Υ. This result shows that our potential which leads to the relation (34) is quite reasonable.(see Table 13.)

* A possible explanation for why we can use nonrelativistic approach to treat all mesons, from light to heavy, has been given by A. Martin [41].

3) In section 3, we found that the hyperfine splitting decrease monotonically with increasing of $m_i + m_j$. A possible way to understand this regularity might be the following. From (12), the hyperfine splitting is

$$M_V - M_P = m_H = (2/3m_i m_j) \langle \nabla^2 V(r) \rangle \qquad (35)$$

where he have omitted the QCD radiative correction factor [38]. Many authors[1), 43), 44)] chose $V(r) \sim -4\alpha_s/3r$ and obtained

$$M_V - M_P = (32\pi/9)(\alpha_s(\mu_{ij}^2)|\psi(0)|^2/\mu_{ij})(m_i + m_j)^{-1} \qquad (36)$$

As suggested by A. Martin [9], expression (36) might be also valid for other phenomenological potentials, since higher derivatives of these potentials may be very different from those of a real potential. So we take (36) as our starting point. Using two-loop QCD expression (26) for running coupling constant, it is easy to show that

$$\alpha_s(\mu_{ij}^2) \cdot \mu_{ij}^{1/2} \simeq \text{const.} \qquad (37)$$

Combining (34) and (37), we obtain

$$\alpha_s(\mu_{ij}^2)\,|\psi(0)|^2/\mu_{ij} \simeq \text{const.} \qquad (38)$$

or more precisely, which depends only slightly on the reduce mass μ_{ij} for $(q_i\bar{Q}_j)$ system. From (38) and (36), we can see that $M_V - M_P$ indeed decrease monotonically with increasing of $m_i + m_j$.

4) For pure strange flavor vector meson $\phi[^3S_1(s\bar{s})]$, From Fig. 2 we predict a pure strange flavor pseudoscalar meson η_s $[^1S_0(s\bar{s})]$ with mass around 720 Mev. But experimentally only the pseudoscalars $\eta(549)$ and $\eta'(958)$ are discovered. We assume that the $|\eta\rangle$ and $|\eta'\rangle$ states are pure $|q\bar{q}\rangle$ and

$$|\eta\rangle = \cos\phi_P\ (|u\bar{u}\rangle + |d\bar{d}\rangle)/\sqrt{2} - \sin\phi_P\ |s\bar{s}\rangle \qquad (39)$$

$$|\eta'\rangle = \sin\phi_P\ (|u\bar{u}\rangle + |d\bar{d}\rangle)/\sqrt{2} + \cos\phi_P\ |s\bar{s}\rangle \qquad (40)$$

where the flavor mixing angle ϕ_P is related to the usual flavor singlet octet mixing angle θ_P by

$$\phi_P = \pi/2 + \theta_P - \tan^{-1}(1/\sqrt{2}) \qquad (41)$$

From (39) and (40), we obtain

$$M[^1S_0(s\bar{s})] = m_\eta + (m_{\eta'} - m_\eta)\cos^2\phi_P$$

using $m_\eta = 549$ MeV, $m_{\eta'} = 958$ MeV and $\theta_P = -11^\circ$ (from masses) or -12° (from two-photon decay of pseudoscalars) [45], we arrive at

$$M[^1S_0(s\bar{s})] \simeq 760 \text{ MeV}$$

which is quite close to our prediction.

ACKNOWLEDGMENTS

The author would like to thank Professor Abdus Salam, the International Atomic Energy Agency and UNESCO for hospitality at the International Centre for Theoretical Physics, Trieste.

REFERENCES

1) E. Eichten et al: Phys. Rev. Lett. 34 369 (1975); 36 500 (1976); Phys. Rev. D17 3090 (1978); D21 203 (1980)

2) T. Appelquist, H.D. Politzer: Phys. Rev. Lett. 34 43 (1975); Phys. Rev. D12 1404 (1975)

3) A. De Rujula, H. Georgi, S.L. Glashow: Phys. Rev. D12 147 (1975)

4) H. Krasmann, S.Ono: Nucl. Phys. B154 283 (1979); S. Ono: Phys. Rev. D20 2975 (1979); D28 558 (1983)

5) G. Bahnot, S. Rudaz: Phys. Lett. B78 119 (1978)

6) C. Quigg, J.L. Rosner: Phys. Rep. C56 168 (1979)

7) J.L. Richardson: Phys. Rev. Lett. B82 272 (1979)

8) H.J. Schnitzer: Phys. Rev. D19 1566 (1979)

9) A. Martin: Phys. Lett. B93 338 (1980)

10) W. Buchmuller: Phys. Rev. Lett. 45 403 (1980)
W. Buchmuller, S.-H.H. Tye: Phys. Rev. D24 132 (1981)

11) D.B. Lichtenberg et al: Phys. Rev. Lett 35 1055 (1975); Z. Phys. C- Particles and Fields 30 103 (1986)

12) P. Mxhoy, J.L. Rosner: Phys. Rev. D28 1132 (1983)

13) P. Falkensteiner et al: Phys. Lett B131 450 (1983)
Z. Phys. C- Particles and Fields 23 275 (1984)

14) S. Godfrey, N. Isgur: Phys. Rev. D32 189 (1985)

15) S.N. Gupta, S.F. Radford: Phys. Rev. D34 201 (1986)

16) X. Song, H. Lin: Z.Phys. C- Particles and Fields 34 223 (1987)

17) A. Martin, Phys. Lett. B100 511 (1981)

18) A. Martin, J.M. Richards: Phys. Lett. B115 323 (1982)

19) R.K. Bhadur et al: Nuovo Cimento 65A 376 (1981)

20) F. Schoberl: Z. Phys. C Particles and fields 15 261 (1982)

21) S.N. Jena: Phys. Rev. D28 2326 (1983)

22) D.B. Lichtenberg, W. Namgung, J.G. Wills, E. Predazzi: Z. Phys. C- Particles and Fields 19 19 (1983)

23) J.L. Basdevant, S. Boukraa: Z. Phys. C28 413 (1985)

24) S.N. Jena, D.P. Rath; Phys. Rev. D32 2366 (1985)

25) Y.J. Ng, J. Pantaleone, S.-H.H. Tye: Phys. Rev. Lett. 55 916 (1985)

26) A.J. Buras:Rev. Mod. Phys. 52 199 (1980); A.H. Mueller:Phys. Rep. 73C 237 (1981); E. Reya: Phys. Rept. 69 195 (1981)

27) K. Igi, S. Ono: Phys. Rev. D33 3349(1986)

28) J. Pantaleone et al: Phys. Rev. D33 777 (1986)

29) Van Royen, E. Weisskopf: Nuovo Cimento 50 617 (1967)

30) M.G. Olsson, C.J. Suchyta III: Phys. Rev. D36 1459 (1987)

31) H.B. Thacker, E. Eichten, J.C. Sexton: FermiLab-Conf-87/204-7

32) D. Gromes: Nucl. Phys. B131 80 (1977)

33) A. Martin: Proc. of the Inter. Conf. in High Energy Physics, Lisbon 1981; Comments Nucl. Part. Phys. 16 249 (1986)

34) M. Frank, P.J. O'Donnel: Phys. Lett 159B 232 (1985)
CERN-TH, 4367/86

35) K. Igi, S. Ono: Phys. Rev. D32 231 (1985)

36) X. Song: Preprint, INPP, Univ. of Virginia, May 1987

37) B. Durand, L. Durand: Phys. Rev D30 1904 (1984)

38) W. Buchmuller, Y.J. Ng, S.-H.H. Tye: Phys. Rev. D24 3003 (1981)

39) R. Babieri, R. Gatto, R. Kogerler: Phys. Lett. B60 183 (1976)

40) R. Babieri et al: Phys. Lett. B61 465 (1976)

41) Y. Hara: Prog. Theor. Phys. 65 1987 (1981)

42) T. Barnes. Proc. of the VIIth Inter. Workshop on Photon-Photon Collisions, Eds. A. Couran and P. Kessler, 1986

43) S. Ishida, K. Yamada: Phys. Rev. D35 265 (1987)

44) S. Jacobs et al: Phys. Rev. D33 3338 (1986)

45) Proc. of the APS-DPF Conf. Eds. J. Ball, (1987)

46) B. Margolis, R.R. Mendel: Phys. Rev. D28 468 (1983)

Table 1. Comparison of the energy levels and of the ratios of leptonic widths with other potential models and with the data for $c\bar{c}$. A * denotes an input used to determine the adjustable parameters.

State	Mas (MeV)						
	Data	This paper	16)	1)	9)	7)	10)
1S	3096.9±0.1	3096.9*	3096.9*	3095*	3095*	3095*	3100*
1P	3521	3520.2	3524.3	3522*	3502	3514	3520
2S	3686.0±0.1	3674.6	3672.5	3684*	3687	3684*	3700
1D	3770.0±3.0	3792.5	3791.2	3810	3787	3799	3810
2P		3914.8	3907.3			3950	3970
3S	4030 ± 5	4031.8	4017.2	4110	4032	4096	4120
2D	4159 ±20	4107.7	4090.4	4190	4092	4172	4190
3P		4208.7	4185.6			4308	
4S	4415 ± 6	4306.3	4275.5	4460	4280	4440	4480
3D		4361.7	4327.6				
4P		4449.6	4409.5				
5S		4535.1	4486.9	4790			
6S		4734.1					
$\Gamma(nS\to e^+e^-)/\Gamma(1S\to e^+e^-)$							
1S	1	1	1	1	1	1	1
2S	0.45±0.08	0.40	0.40	0.44	0.40	0.45	0.46
3S	0.16±0.04	0.25	0.24	0.31	0.25	0.32	0.32
4S	0.11±0.04	0.18	0.17	0.23	0.16	0.24	0.25
5S		0.15	0.14	0.17			
6S		0.13					

Table 2. Comparison of the energy levels and of the ratios of leptonic widths with the data and with other potential models for $b\bar{b}$. A * denotes an input used to determine the adjustable parameters

States	Mass(MeV)						
	Data	This paper	16)	1)	9)	7)	10)
1S	9460.0±1.3	9460.0*	9460.0*	9460*	9460*	9452*	9460*
1P	9900 ±3	9892.6	9902.0	9960	9861	9888	9890
2S	10023.4±0.3	10024.0	10034.4	10050	10025	10007	10020
1D		10149.2	10161.6	10200		10137	10140
2P	10256 ±5	10250.0	10260.6	10310	10242	10241	10250
3S	10355.5±0.5	10352.0	10355.8	10400	10360	10338	10350
2D		10426.3	10432.5	10500		10421	10430
3P		10506.5	10512.3	10600		10512	10530
4S	10577 ±4	10586.4	10588.9	10670	10600	10598	10620
3D		10641.6	10642.7	10750			10680
4P		10712.6	10710.9				
5S	10868 ±8	10781.5	10776.0	10920	10760		10860
6S	11019 ±9	10949.1					
$\Gamma(nS\to e^+e^-)/\Gamma(1S\to e^+e^-)$							
1S	1	1	1	1	1	1	1
2S	0.46±0.03	0.44	0.43	0.36	0.51	0.42	0.44
3S	0.33±0.03	0.30	0.28	0.25	0.35	0.30	0.32
4S	0.19±0.03	0.23	0.22	0.20	0.27	0.27	0.26
5S	0.14±0.01	0.19	0.18		0.21		
6S		0.17					

Table 3. Prediction of the energy levels

State	Mass(GeV)		
	m_t=40	m_t=45	m_t=50
1S	78.790	88.726	98.667
1P	79.372	89.324	99.279
2S	79.494	89.446	99.402
2P	79.746	89.702	99.583
3S	79.825	89.781	99.741
4S	80.045	90.003	99.963
5S	80.212	90.169	100.131

Table 4. Comparison of the energylevels with the data and with other potential models for $u\bar{u}$, $d\bar{d}$, $u\bar{s}$ and $s\bar{s}$

state	Data (MeV)	This paper	14)	43)	16)
ρ	770±3	770*	770*	763*	
ρ'	1590±20	1535.1	1450	1600	
ρ''	2150	2036.7	2000	2140	
a_0	983±3	909.6	1090	940	
a_1	1275±28	1266.9	1240	1240	
a_2	1318±5	1433.4	1310	1300	
ρ_3	1691±5	1688.4	1700	1690	
K*	892.1±0.3	892*	900*	898*	
K*'	1650	1632	1580	1670	
K*"		2107	2110	2190	
ϕ	1019.5±0.1	1019.5*	1020*	1020*	1019.5*
ϕ'	1685 $^{+75}_{-15}$	1729.8	1690	1740	1684.8
ϕ''		2174.6		2250	2101.0
f_0	1300	1284.9	1360	1180	
f_1	1422 ±10	1488.7	1480	1430	
f_2	1525 ±5	1620.8	1480	1530	

Table 5. Comparison of the first two levels with the data and with other potential models for $c\bar{u}$, $c\bar{s}$, $b\bar{u}$, $b\bar{s}$ and $b\bar{c}$

State	Data (MeV)	This paper	14)	23)
($c\bar{u}$)				
D^*	2010.1±0.7	2010	2040	1983
$D^{*'}$		2734	2630	2614
($c\bar{s}$)				
D_s^*	2140 ±60	2140	2130	2088
$D_s^{*'}$		2824	2730	2718
($b\bar{u}$)				
B^*	5325	5325	5370	5260
$B^{*'}$		6044	5930	5845
($b\bar{s}$)				
$B_s^{*'} - B_s^*$		597	560	588
($b\bar{c}$)				
$B_c^{*'} - B_c^*$		567	550	571

Table 6. Comparison of the fine splittings of n^3P_J states with experiment for $c\bar{c}$ and $b\bar{b}$, and the prediction for $t\bar{t}$ (m_t=45 GeV)

		$c\bar{c}$(MeV)		$b\bar{b}$(MeV)		$t\bar{t}$ (GeV)
State	J	Data	Theor.	Data	Theor.	Theor.
1^3P_J	0	3415.0±1.0	3454.8	9872.9±5.8	9866.2	89.315
	1	3510.0±0.6	3506.5	9894.5±3.5	9890.6	89.321
	2	3555.8±0.6	3543.8	9914.6±2.4	9910.0	89.327
2^3P_J	0		3884.8	10233.0±3.0	10228.4	89.697
	1		3921.1	10253.7±3.4	10244.4	89.701
	2		3946.2	10271.0±2.4	10257.1	89.704
3^3P_J	0		4171.2		10489.9	89.938
	1		4200.5		10502.4	89.941
	2		4221.1		10512.3	89.943

Table 7. Comparison of a_P and b_P with the data for $c\bar{c}$ and $b\bar{b}$

		data	theor.			data	theor.
1^3P_J(cc)	a_p	34.0±1.0	23.2	2^3P_J(cc)	a_p		16.3
	b_p	10.0±1.0	4.7		b_p		3.3
(bb)	a_p	13.0±1.0	12.1	(bb)	a_p	11.0±2.0	8.0
	b_p	2.5±0.3	2.1		b_p	1.7±1.0	1.4

Table 8. Comparison of the hyperfine splittings with the data and other potential models

State	Data (MeV)	This paper	14)	43)	24)
$\rho - \pi$	$630.43_{635.04}\pm 3$	608	620	623	
$\rho' - \pi'$	330 ± 100	332	150	330	
$K^* - K$	$398.4_{394.3}\pm 0.3$	399	430	404	
$K^{*\prime} - K'$	~230	212	130	310	
$\phi - \eta_s$	[260]	318		330	
$\phi' - \eta_s'$		161		300	
$D^* - D$	$140.8_{142.6}\pm 2.1$	162	160		
$D^{*\prime} - D'$		84	60		
$D_s^* - D_s$	139.5 ± 18 144.0 ± 16	148	150		
$D_s^{*\prime} - D_s'$		76	60		
$J/\psi - \eta_c$	115.9 ± 2	76.2	140		117
$\psi' - \eta_c'$	96	37.5	60		60
$B^* - B$	52 ± 6	55.6	60		
$B^{*\prime} - B'$		28	30		
$B_s^* - B_s$		47.6* (78**)	60		
$B_s^{*\prime} - B_s'$		25	30		
$B_c^* - B_c$		42	70		
$B_c^{*\prime} - B_c'$		20	40		
$\Upsilon - \eta_b$		33.7	60		29
$\Upsilon' - \eta_b'$		14.5	20		14
$T - \eta_t$		6.8	30		
$T' - \eta_t'$		2.1	10		

* b=0.42 in V(r)

** b=0.60 in V(r)

Table 9. Comparison of the 2γ, 3γ, $2g$, $3g$ and $2g+\gamma$, decay rates with the data and other models for $u\bar{u}$, $s\bar{s}$, $c\bar{c}$ and $b\bar{b}$.

Decay	Data	This paper	16)	14)	44)
$\eta' \to 2\gamma$	4.56 kev	4.26 kev			
$\eta_c \to 2\gamma$	9 ± 4 kev	13.21 kev	6.54 kev	6.76kev	
$\eta_b \to 2\gamma$		0.49 kev	0.33 kev		
$\rho \to 3\gamma$		$3.4\ 10^{-3}$kev			
$\phi \to 3\gamma$		$20.1\ 10^{-3}$kev			
$J/\psi \to 3\gamma$	0.004 kev	0.008 kev	0.0024kev		
$\psi' \to 3\gamma$	0.0008 kev	0.002 kev	0.0008kev		
$\psi' \to 3\gamma / J/\psi \to 3\gamma$	0.20	0.25	0.33		
$\Upsilon \to 3\gamma$		$4.8\ 10^{-5}$kev	$2.6\ 10^{-5}$		
$\Upsilon' \to 3\gamma$		$2.1\ 10^{-5}$kev	$1.1\ 10^{-5}$		
$\eta_c \to 2g$	11.5 ± 4.0MeV	11.88 MeV	6.71 MeV	22.1MeV	11.5MeV
$\eta_b \to 2g$		4.43 MeV	3.07 MeV		4.7MeV
$\eta_c \to 2g / \eta_c \to 2\gamma$	$(1.2\pm0.5)\ 10^3$	$0.9\ 10^3$	$1.0\ 10^3$		
$J/\psi \to 3g$	45 ± 12 kev	115.5 kev	69.88 kev	176 kev	
$J/\psi \to 3g / J/\psi \to 3\gamma$	$(1.1\pm0.3)\ 10^4$	$1.4\ 10^4$	$2.9\ 10^4$		
$\psi' \to 3g$	18 kev	39.7 kev	23.67 kev	78.4kev	
$\psi' \to 3g / \psi' \to 3\gamma$	$(2.3\ )10^4$	$2.0\ 10^4$	$3.0\ 10^4$		
$J/\psi \to 3g / \psi' \to 3g$	2.5 ± 0.7	2.90	2.95		
$\Upsilon \to 3g$	42.5 ± 4.0kev	36.5 kev	26.0 kev	44.1kev	
$\Upsilon' \to 3g$		15.6 kev	10.7 kev	22.5kev	
$J/\psi \to 2g+\gamma$	6.3 kev	13.5 kev	9.8 kev		
$\Upsilon \to 2g+\gamma$	1.3 ± 0.4kev	1.3 kev	1.1 kev		
$J/\psi \to 3g/\gamma / J/\psi \to 2g+\gamma$	7.1 ± 1.9	8.5	7.1		
$\Upsilon \to 2g+\gamma / \Upsilon \to 3g$	(2.99 ± 0.59)%	3.56%	4.24%		

Table 10. Comparison of the 2g and 3g decay rates with the data and with other model for χ_c and χ_b (1^3P_J)

decay	data [45)44)]	This paper	44)
$\chi_{0c} \to 2g$		2.36 MeV	
$\chi_{1c} \to 3g$		65.5 keV	
$\chi_{2c} \to 2g$	2.5±1.0 MeV	0.67 Mev	0.70 MeV
$\chi_{0b} \to 2g$	379 keV	393.4 keV	
$\chi_{1b} \to 3g$	50 keV	35.3 keV	
$\chi_{2b} \to 2g$	122 keV	104.9 keV	123 keV
	(144±35 keV)		

Table 11. Comparison of the E_1 and M_1 transition rates with data and other models for $c\bar{c}$ and $b\bar{b}$ (all units are keV)

	E_1	J	Data	ours	16)	1)	9)	10)	7)
$c\bar{c}$	$1^3P_J \to 1^3S_1$	2	555±130	403.0	381	398	394	496	497
		1	405	320.0	309	289	295	381	372
		0	96± 46	217.6	218	141	141	182	178
	$2^3S_1 \to 1^3P_J$	2	17±1.7	35.3	31	33	33	38	39
		1	19±1.7	42.2	36	45	45	49	54
		0	20±1.7	30.3	26	50	51	58	61
$b\bar{b}$	$1^3P_J \to 1^3S_1$	2		36.4	36	26	36	34.5	34
		1		32.0	32	20	28	34.5	26
		0		26.9	27	13	18	34.5	17
	$2^3S_1 \to 1^3P_J$	2	2.07±0.24	2.65	2.6	3.1	2.4	2.1	3.1
		1	2.01±0.24	2.47	2.3	4.3	3.3	2.1	4.2
		0	1.18±0.24	1.32	1.2	3.4	2.6	2.1	3.3
	M_1								
$c\bar{c}$	$1^3S_1 \to 1^1S_0$		0.57-1.03	2.21	1.47	1.51	1.58		2.31
	$2^3S_1 \to 2^1S_0$		0.43-2.80	1.27	0.99	1.11	1.16		1.69

Table 12. Prediction of E_1 transition rates for $t\bar{t}$

Transition	J	Γ(keV)		
		m_t=40(GeV/c^2)	m_t=45	m_t=50
$1^3P_J \to 1^3S_1 + \gamma$	2	30.70	28.60	26.90
	1	29.60	27.80	26.20
	0	28.60	26.90	25.40
$2^3P_J \to 2^3S_1 + \gamma$	2	8.94	8.73	7.49
	1	8.62	7.85	7.24
	0	8.22	7.49	6.99
$2^3P_J \to 1^3S_1 + \gamma$	2	8.49	7.95	4.01
	1	8.41	7.87	3.97
	0	8.31	7.78	3.91
$2^3S_1 \to 1^3P_J + \gamma$	2	1.19	1.07	0.97
	1	0.85	0.74	0.66
	0	0.33	0.28	0.26
$3^3S_1 \to 2^3P_J + \gamma$	2	1.06	0.94	0.84
	1	0.71	0.63	0.56
	0	0.28	0.24	0.21

Table 13. Comparison of Γ_{ee}/e_Q^2 with the data for ρ, ω, ø, J/ψ and ϒ, and prediction for $T(t\bar{t})$

state	M_V(MeV)	Γ_{ee} (keV)	e_Q^2	Γ_{ee}/e_Q^2 (keV)		
				Data	ours	46)
ρ	770	6.9±0.3	1/2	13.80±0.60	13.12	15.60
ω	783	0.66±0.04	1/18	11.88±0.72	12.60	15.12
ø($s\bar{s}$)	1020	1.31±0.06	1/9	11.79±0.54	11.79*	15.26
J/ψ($c\bar{c}$)	3100	4.7±0.3	4/9	10.58±0.68	11.10	
ϒ($b\bar{b}$)	9460	1.22±0.05	1/9	10.98±0.45	10.03	
$T(t\bar{t})$	88726		4/9		5.40	

Figure captions:

Fig. 1 The $M_V^2 - M_P^2 = \text{Constant} \times \alpha_s(\mu_{ij}) |\psi(0)|^2 / \mu_{ij}$ is plotted as a function of the reduced mass μ_{ij}. Data for $k^{*2} - k^2$ is used as an input.

Fig. 2 The $M_V - M_P$ (see eq.(36)) is plotted as a function of the sum of the constituent quark mass.

Fig. 3 The $M_V - M_P$ is plotted as a function of the reduced mass μ_{ij}.

Fig. 4 The $|\psi(0)|^2$ predicted in our model is plotted as a function of reduced mass μ_{ij}.

Fig. 5 The Γ_{ee}/e_Q^2 predicted in our model is plotted as a function of the mass of the vector meson. Data for Ø-meson is used as an input.

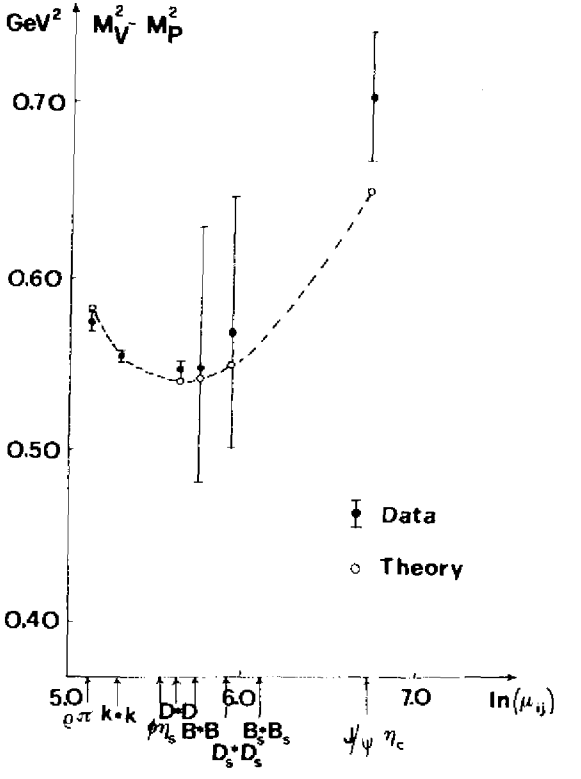

Fig.1

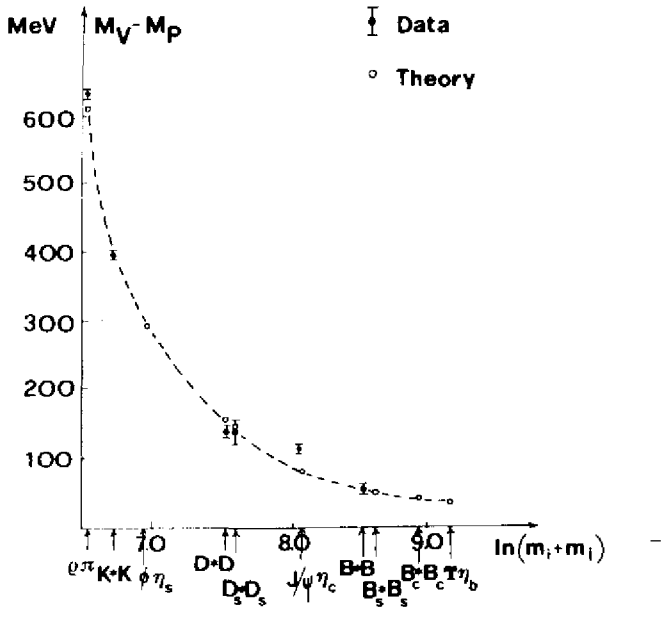
MeV
$M_V - M_P$
Data
Theory
600
500
400
300
200
100
7.0
8.0
9.0
$\ln(m_i+m_j)$
$\varrho\pi$
K*K
$\phi\eta_s$
D*D
$D_s^*D_s$
$J/\psi\eta_c$
B*B
$B_s^*B_s$
$B_c^*B_c$
$T\eta_b$

Fig.2

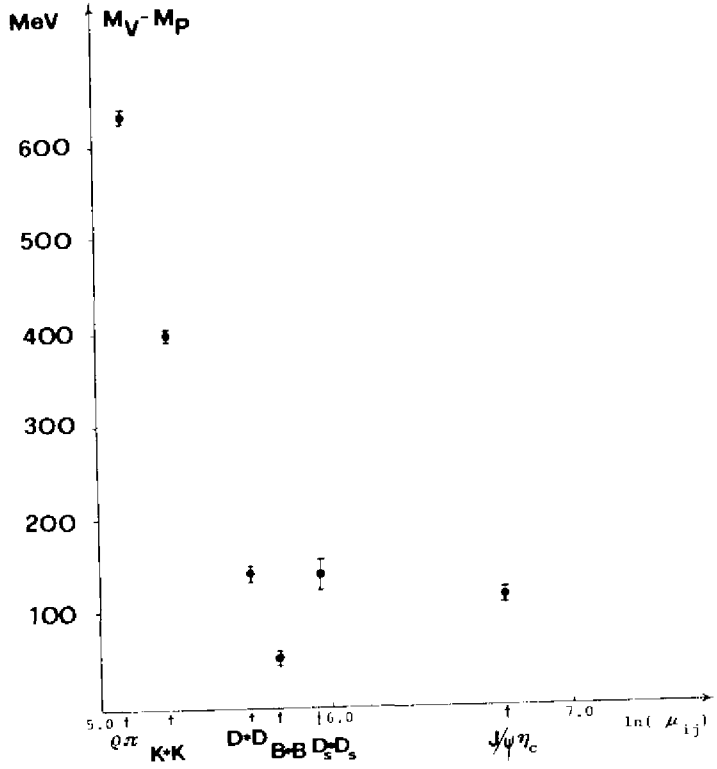
MeV
$M_V - M_P$
600
500
400
300
200
100
5.0
6.0
7.0
$\ln(\mu_{ij})$
$\varrho\pi$
K*K
D*D
B*B
$D_s^*D_s$
$J/\psi\eta_c$

Fig. 3

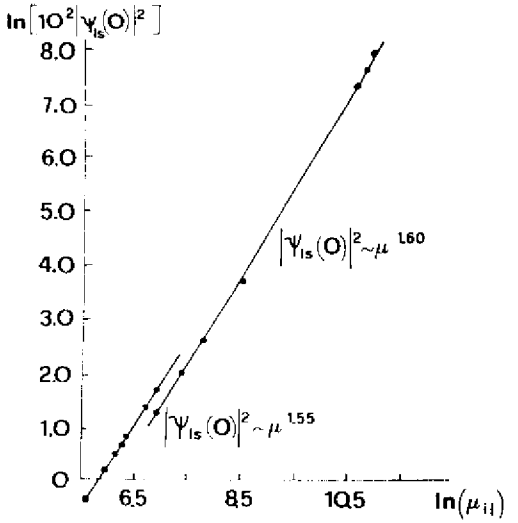
$\ln\left[10^2|\psi_{1s}(0)|^2\right]$
8.0
7.0
6.0
5.0
4.0
3.0
2.0
1.0
0
$|\psi_{1s}(0)|^2 \sim \mu^{1.60}$
$|\psi_{1s}(0)|^2 \sim \mu^{1.55}$
6.5
8.5
10.5
$\ln(\mu_{ij})$

Fig.4

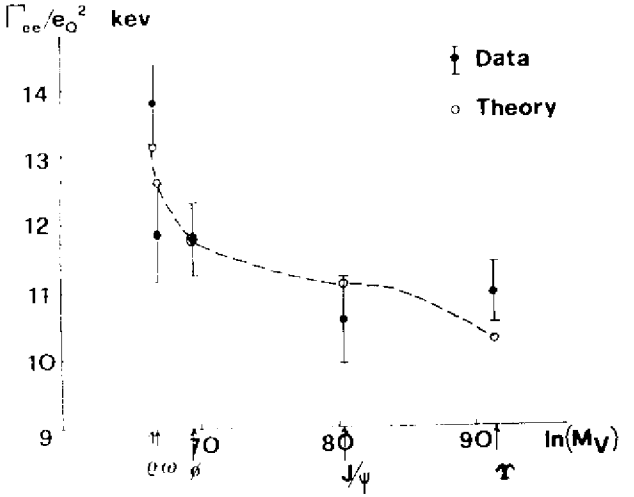
Γ_{ee}/e_Q^2 kev
Data
Theory
14
13
12
11
10
9
7.0
8.0
9.0
$\ln(M_V)$
$\rho\omega$
ϕ
J/ψ
Υ

Fig.5

Stampato in proprio nella tipografia
del Centro Internazionale di Fisica Teorica